JOC The Journal of Organic Chemistry
Cite This: J. Org. Chem. 2019, 84, 8571−8577
Article
pubs.acs.org/joc

Fluorescent Arylethynyl Hamilton Receptors for Barbiturate Sensing

Daniel T. Seidenkranz and Michael D. Pluth*

Department of Chemistry and Biochemistry, Materials Science Institute, University of Oregon, Eugene, Oregon 97403, United States

Supporting Information

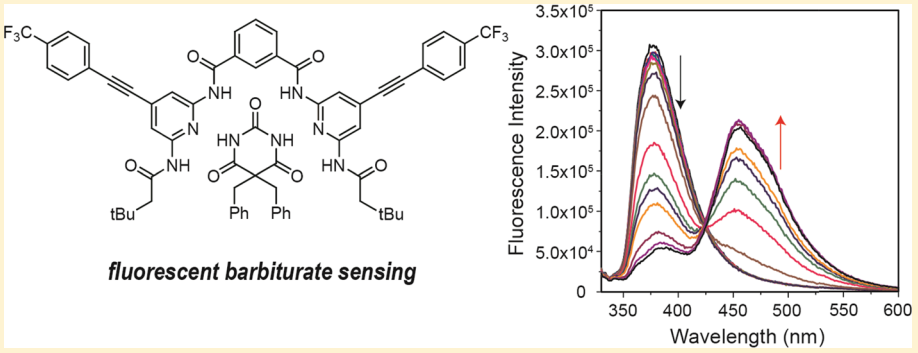

ABSTRACT: Barbiturates are common targets for molecular recognition in preorganized receptors due to complementary hydrogen-bond donor/acceptor interactions. Although many such receptors exhibit high selectivity and affinity for barbiturate guests, relatively few of these systems have desirable photophysical properties for sensing applications. Here, we report the synthesis, optoelectronic properties, and binding affinities of a suite of fluorescent arylethynyl Hamilton receptors. We also provide insights into the design principles required for efficient fluorogenic design of these systems to function as fluorescent barbiturate sensors.

INTRODUCTION

Hydrogen bonding is a ubiquitous theme in the fields of self-assembly and molecular recognition. Owing to the high directionality of H bonds, host−guest systems incorporating these types of noncovalent interactions often exhibit significant cooperativity leading to strong association constants. Of the numerous host−guest architectures that incorporate hydrogen bonding as the primary recognition motif,[1] one of the most ubiquitous scaffolds is that based on the synthetic barbiturate receptor developed by Chang and Hamilton (Figure 1).[2]

This highly utilized class of macrocyclic 2,6-diamidopyridine receptors is characterized by the two symmetric donor−acceptor−donor H-bonding schemes of the host that align with the two symmetric acceptor−donor−acceptor H-bonding schemes of barbiturates. These types of systems exhibit large association constants (K_a) for barbituric acid derivatives ranging from 10^5 to 10^6 M^{-1} in aprotic solvents such as $CHCl_3$ and CH_2Cl_2.[2,3] Although the preorganization imposed by the macrocyclizing component is required for the largest binding affinities, nonmacrocyclic forms of the receptor also display relatively large binding affinities (~10^4 M^{-1}).[3] Our group has previously investigated the impacts of steric[4] and electronic[5] effects on nonmacrocyclic Hamilton receptors. Similarly, other groups have also utilized different acyclic derivatives for a variety of applications including the construction of supramolecular dendrimers[6,7] and polymeric materials,[8−10] utilization as optoelectronic materials,[11−14] and sensing.[15−17]

Although many of these receptors exhibit high selectivity and affinity for barbiturate guests, relatively few of these systems have desirable photophysical properties for sensing applications (e.g., low energy absorbances, strong emission profiles, etc.). Therefore, derivatized Hamilton receptors that contain fluorogenic and other chromophoric groups are needed. Toward these aims, prior work by Aoki et al. demonstrated that appending pyrene moieties to an acyclic Hamilton receptor results in a strong fluorescence turn-on that can be monitored by fluorescence spectroscopy.[18] The efficacy of this system is largely due to solvent effects that cause disaggregation of the host molecule in the presence of barbiturates. Chambers et al. have shown that cholesteryl-modified Hamilton receptors can be incorporated into liquid crystal display technologies that respond with relatively large changes in maximum reflectance wavelengths in the presence of barbital.[19] Other approaches for barbiturate detection include electrochemical methods[20] and Fe spin-crossover complexes that in the presence of barbiturates produce a visible colorimetric response that is selective for barbiturates over structural analogues.[21]

More recently, the Kondo group demonstrated that the appendage of a phenylethynyl group on the 4-position of the isophthalimide backbone results in a turn-on fluorescent probe for barbiturates.[22] While simultaneously working on a similar

Received: April 9, 2019
Published: June 12, 2019

DOI: 10.1021/acs.joc.9b00978
J. Org. Chem. 2019, 84, 8571−8577

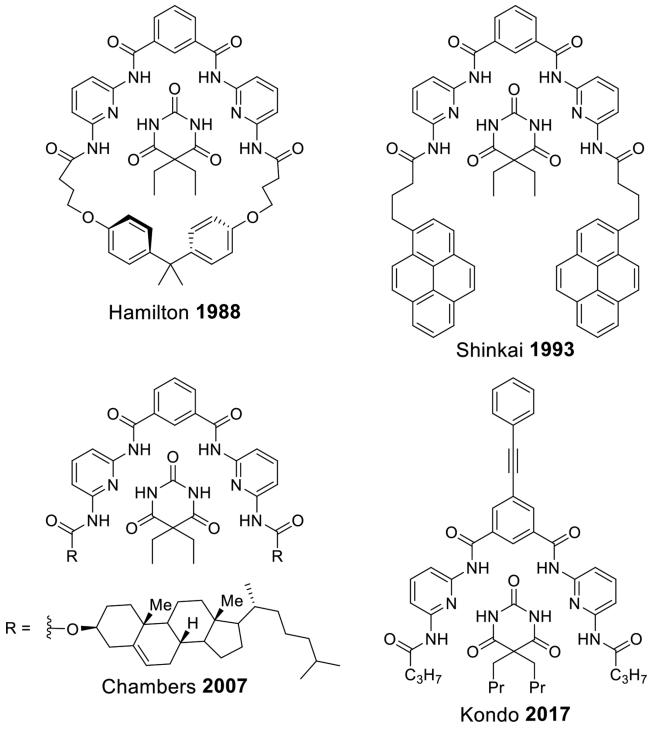

Figure 1. Structures of original and selected modified Hamilton receptors.

design strategy, we hypothesized that appending arylethynyl groups to the 4-position of the diamidopyridine backbone would have two positive effects over the isophthalyl linkage. First, the turn-on response could be easily tuned through the identity of the R-group due to the inherent "push-pull" nature of the fluorophore and greater differences in the ground and excited electronic states between the bound and unbound receptors. Second, the binding affinities of the receptor could be tuned through the incorporation of electron-donating groups or electron-withdrawing groups in the 4-position of the arylethynyl moiety, thereby changing the basicity of the pyridyl nitrogen lone pair. Herein, we report the synthesis, optoelectronic properties, and binding affinities of a suite of arylethynyl Hamilton receptors that function as fluorescent barbiturate sensors and provide insights into the design principles required for efficient fluorogenic properties in Hamilton-based receptors.

RESULTS AND DISCUSSION

The synthesis of the new arylethynyl-containing Hamilton receptors is relatively straightforward. We envisioned that a variety of arylethynyl groups could be appended under typical Sonogashira cross-coupling conditions using the corresponding 4-bromopyridyl precursor (**2**). Using methods similar to those reported previously,[4,23] we were able to prepare the brominated analogue of a typical acyclic Hamilton receptor **2**. This precursor was then subjected to standard Sonogashira cross-coupling conditions to yield the final products in moderate yields from commercially available materials (Scheme 1). Purification of these molecules could be obtained through column chromatography or in some cases recycling GPC to remove any unreacted starting material or mono-substituted products. Using this methodology, we prepared a variety of 4-substituted arylethynyl Hamilton receptors that included strongly electron-donating and strongly electron-withdrawing groups (**3a**–**e**).

With these new receptors in hand, we first examined their optical properties (Table 1). The absorption maxima of **3a**–**e** range from 321 to 368 nm with receptor **3e** showing the most red-shifted absorption. As we hypothesized, the emission spectra exhibit notable differences upon substitution of the arylethynyl moiety (Figure 2a). Receptors **3a**–**d** exhibited very weak emission profiles in the absence of the guest. In contrast, **3e** shows a strong emission maximum at 451 nm in the absence of the guest. This change in emission behavior is likely due to the charge transfer between the strongly electron-donating dimethylamino group and electron-poor pyridine ring, which was observed in other push-pull pyridine-containing systems.[24,25]

Further supporting the charge transfer behavior, we also observed that receptors **3a**–**d** displayed solvatochromic properties common to other charge transfer systems in both the absorbance (Figure S2) and fluorescence spectra (Figure 3). In addition to the absorbance and emission bathochromic shifts, the fluorescence intensity decreases as the solvent polarity increases (Figure S3). This behavior has been exhibited in other fluorogenic charge transfer systems and is caused by the increase in nonradiative pathways available in

Scheme 1. Synthesis of Substituted Arylethynyl Hamilton Receptors

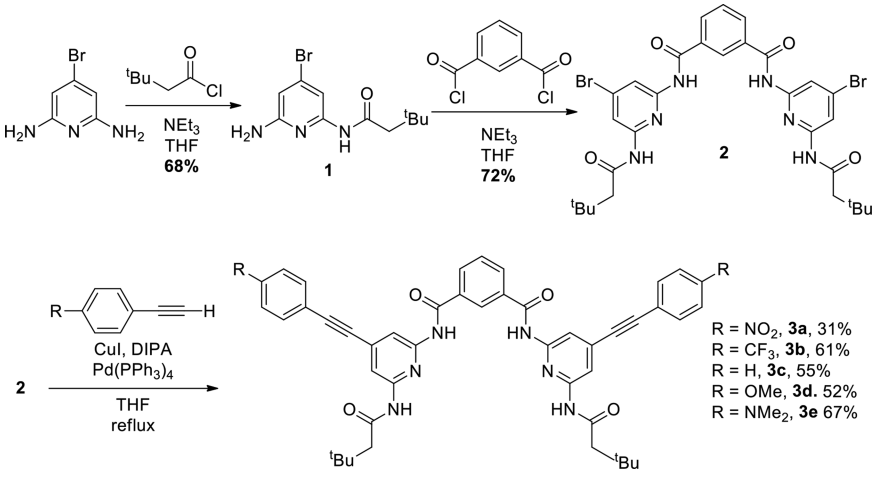

DOI: 10.1021/acs.joc.9b00978
J. Org. Chem. 2019, 84, 8571–8577

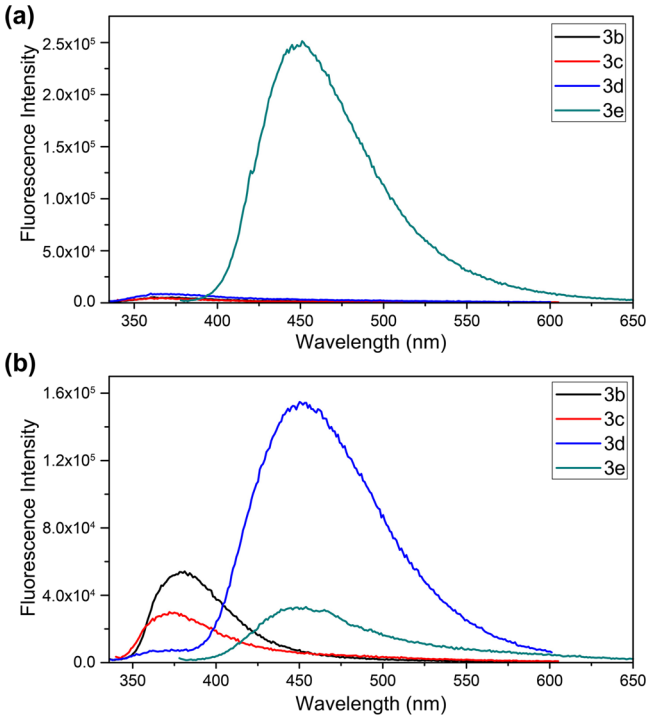

Figure 2. (a) Emission spectra of hosts **3b**−**e** (1 μM) in H_2O-saturated $CHCl_3$. (b) Emission spectra of hosts **3b**−**e** (1 μM) in the presence of 200 equiv of **4b** in H_2O-saturated $CHCl_3$.

Table 1. Photophysical Properties of Hosts 3a−e in the Presence and Absence of Barbital Guest[a]

host	λ_{max} (nm)	ε ($\times 10^4$ M^{-1} cm^{-1})	λ_{em} (nm)
without barbital			
3a	321	7.68 ± 0.03	
3b	303	7.36 ± 0.02	
3c	306	9.04 ± 0.05	
3d	324	8.27 ± 0.06	
3e	368	7.6 ± 0.1	451
with barbital			
3a	321		
3b	305		380
3c	306		372
3d	327		449
3e	374		454

[a] λ_{max} measured with [H] = 5 μM in H_2O-saturated $CHCl_3$. ε measured in H_2O-saturated $CHCl_3$. λ_{em} in the presence of barbital measured with [H] = 1 μM in H_2O-saturated $CHCl_3$ and 200 equiv of barbital.

the excited state that is stabilized by the polar solvent molecules.[26]

With the photophysical properties of new hosts **3a**−**e** being measured, we sought to probe the changes of these photophysical properties to the addition of guest molecules. Previously reported systems based on unsubstituted arylethynyl systems show a turn-on fluorescence response to the addition of barbiturate guests, in addition to small changes in the absorption spectra.[22] We observed similar spectral changes for our substituted arylethynyl hosts upon the addition of barbital (Figure S4). The absorption spectra show small red-shifts ranging from 3 to 6 nm upon the addition of barbital (Figure S4), while the changes in the emission spectra are

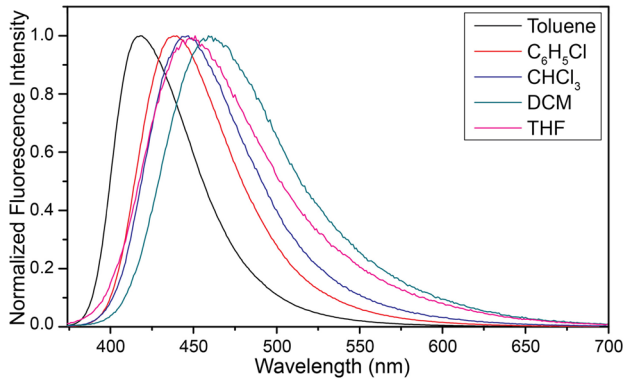

Figure 3. Emission spectra of **3e** in different solvents ([**3e**] = 5 μM, λ_{ex} = absorbance λ_{max} for the given solvent).

much more dynamic. Unsurprisingly, the fluorescence of **3a** remains quenched due to the presence of the nitro group. However, other electron-withdrawing substituents such as the CF_3 moiety of **3b** show a moderate fluorescence turn-on (6.7-fold) at 380 nm upon the addition of barbital. Similar behavior is exhibited for the H-substituted receptor **3c** (4.9-fold turn-on). Upon increasing to more electron-donating substituents, a dramatic red-shifting in the emission profile occurs with receptor **3d** exhibiting an λ_{em} of 449 nm in addition to a much stronger fluorescence turn-on (17-fold). In contrast, the even more electron rich NMe_2 substituted receptor **3e** shows a turn-off response to the addition of barbital.

To explain the quenching effect observed for **3e** in the presence of barbital, we reasoned that protonation of the dimethylamino group by the barbiturate N−H could be responsible. Using ^1H NMR spectroscopy, we performed a titration experiment with barbital and **3e** in H_2O-saturated $CDCl_3$. However, upon increasing the amount of guest, there was no observable change in the dimethylamino resonance indicating that protonation of the group did not occur. Instead, typical down-field shifts are observed for the two amide N−H groups (Figure 4).

To further probe the differences between the emission profiles of our receptors, we hypothesized that protonation of the pyridyl nitrogen could be responsible for the emission feature at 445 nm. Therefore, the emission profiles of electron-poor receptors, such as **3b**, could be caused by weak proton transfer between the barbiturate N−H and the pyridine. To determine the effect of protonation at the pyridyl nitrogen, we performed fluorescence titration between receptor **3b** and dibenzylbarbital (**4d**) followed by addition of acetic acid. Upon addition of barbital, we observed a fluorescence turn-on at 380 nm. Interestingly, the subsequent addition of acetic acid to the same solution containing **3b** and **4d** yields a ratiometric response with an increasing emission band at 453 nm and a decrease in the band at 380 nm. (Figure 5). An isosbestic point is observed at 425 nm confirming a direct conversion of the H−G complex to the protonated host complex.

After determining the photophysical properties of our new receptor library, we wanted to determine the effect of the R group on the binding of barbital. Fluorescence titrations were performed, and the total integrated fluorescence data were fit to a 1:1 binding model. The results are summarized in Table 2 and are similar to those reported previously for similar systems.[22] As we hypothesized, the binding affinities could be tuned through substitution of the R group on the arylethynyl

DOI: 10.1021/acs.joc.9b00978
J. Org. Chem. 2019, 84, 8571−8577

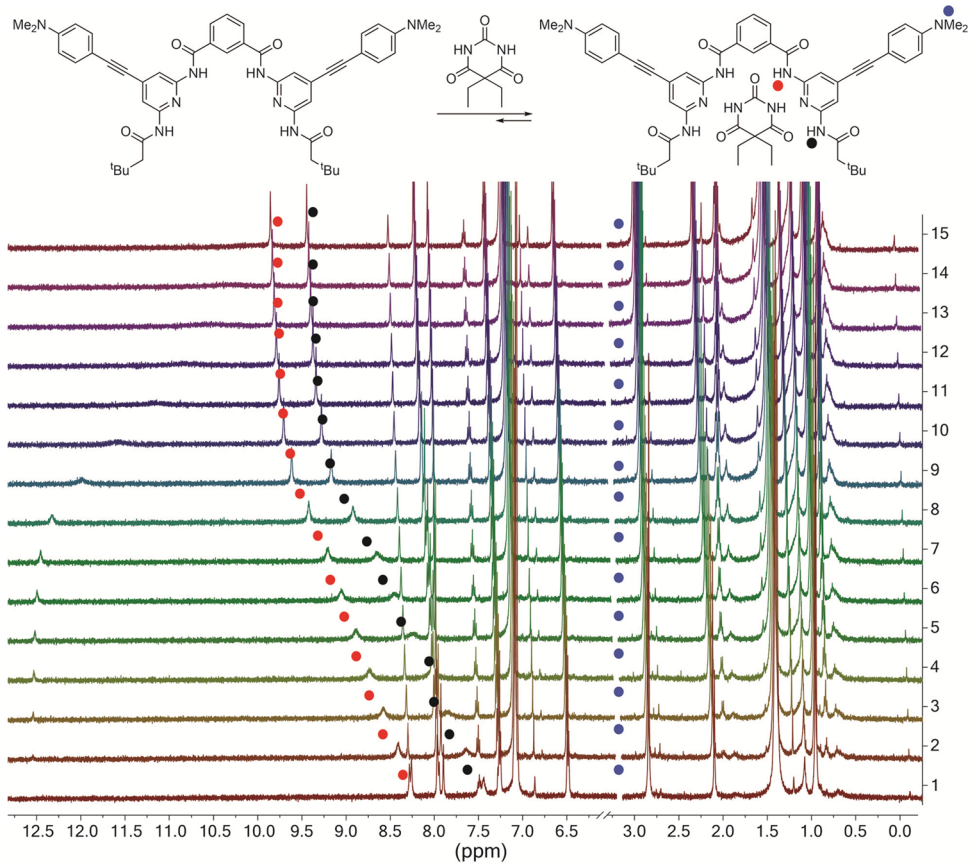

Figure 4. ^{1}H NMR (500 MHz) titration of **3e** with barbital (**4b**) in H_2O-saturated $CDCl_3$ at 25 °C.

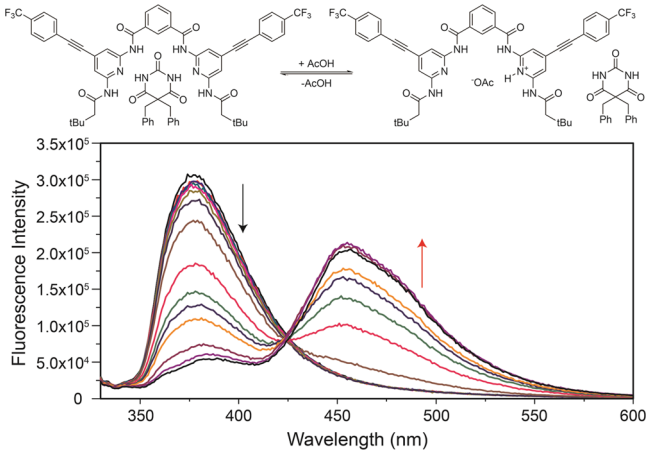

Figure 5. Emission spectra of **3b** in the presence of **4d** showing a ratiometric response to the addition of AcOH.

Table 2. Binding Affinities of Hosts 3b–e with Barbital at 25 °C in H_2O-Saturated $CHCl_3$[a]

host	K_a ($\times 10^4$ M^{-1})
3b	3.04 ± 0.04
3c	3.3 ± 0.2
3d	3.80 ± 0.06
3e	4.0 ± 0.03

[a]The error is shown as ±σ.

moiety. Electron-donating groups effectively increase the basicity of the nitrogen lone pair, making the system a better H-bond acceptor, while electron-withdrawing groups decrease the pyridyl lone pair basicity leading to a lower binding affinity.

We next constructed a Hammett plot from the titration data to determine whether this system exhibits a linear free energy relationship. The data show a moderately correlated linear trend (Figure S5). The negative slope (ρ = −0.10) is indicative of an increase in the positive charge upon barbiturate binding, corroborating the partial proton transfer between the barbiturate N–H and pyridyl nitrogen. The magnitude of the slope indicates that the R groups have a weak influence on the binding affinity of the guests and is likely due to the relatively large distance between the R group and the pyridyl nitrogen.

In addition, we also investigated whether barbiturate substitution impacted binding to the receptor motifs. We chose receptor **3b** as the model host and measured the change in fluorescence upon titration with guests **4a–d** (Figure 6). Although the size of these barbiturates changed significantly,

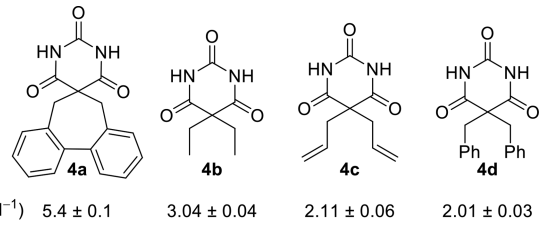

Figure 6. Binding affinities of guests **4a–e** and receptor **3b** at 25 °C in H_2O-saturated $CHCl_3$. Binding isotherms are fit to a 1:1 binding model. The error is shown as ± σ.

DOI: 10.1021/acs.joc.9b00978
J. Org. Chem. 2019, 84, 8571–8577

there were no large changes or correlations between the size of the barbiturate and binding affinity. We did observe, however, that guest **4a** exhibited a 2-fold stronger binding than other guests, which we attribute to the locked conformation of the 5,5′ groups on the barbiturate, which help preorganize the guest to have minimal negative steric interactions with the distal neopentyl groups of the host.

CONCLUSIONS

In summary, we have prepared a small library of substituted arylethynyl Hamilton receptors via simple Sonogashira coupling in moderate yields. These new receptors exhibit tunable photophysical properties dependent on the identity of arylethynyl substituents. Electron-withdrawing substituents show a moderate fluorescence turn-on in the presence of barbiturate guests with λ_{em} between 372 and 380 nm. Electron-donating substituents exhibit bimodal behavior. In the case of the OMe-substituted host (**3d**), a stronger, red-shifted fluorescence turn-on at 449 nm is observed. In contrast, the most electron-donating NMe_2 host (**3e**) shows a turn-off fluorescence response in the presence of the guest. Additionally, the fluorescence of this compound exhibits mild solvatochromic behavior. The binding affinity of these receptors toward barbiturates can be modulated with a moderate impact by the electron-donating/-withdrawing nature of the arylethynyl substituents and exhibits a moderately correlated linear free energy relationship. Overall, these findings demonstrate the fine control of photophysical and binding properties that can be achieved through careful tailoring of the electronics of appended fluorophores to acyclic Hamilton receptors. Specifically, the electron density at the pyridyl nitrogen plays an important role in both the optical properties and guest binding.

EXPERIMENTAL SECTION

General. All commercially available reagents were used as received. Anhydrous, deoxygenated solvents were collected from a Pure Process Technologies solvent purification system. Triethylamine was dried and distilled over CaH_2 under nitrogen. Barbiturates were synthesized according to the procedures outlined in Syntheses of this paper. Reactions were monitored using Merck F_{254} silica gel 60 TLC plates and visualized using UV light or a $KMnO_4$ stain. Reactions conducted under an inert atmosphere were performed by using standard Schlenk techniques. Chromatographic purification was performed using a Biotage automated flash chromatography purification system. Preparative HPLC chromatography was performed using a JAI Recycling Preparative HPLC (Model LC-9101) with a JAIGEL-1H preparative column. ^1H and $^{13}C\{^1H\}$ NMR spectra were recorded at the reported frequencies, and chemical shifts are reported in ppm (δ) and referenced to the residual solvent resonance. $^{31}P\{^1H\}$ chemical shifts are referenced to H_3PO_4. The following naming conventions were used to describe NMR couplings: (s) singlet, (d) doublet, (t) triplet, (q) quartet, (dd) doublet of doublets, (m) multiplet, and (b) broad. Mass spectrometric measurements were performed by the University of Illinois, Urbana Champaign MS Facility, or on a Waters Xevo ESI LC/MS instrument. Absorbance measurements were performed using an Agilent Technologies Cary 60 spectrometer. Fluorescence measurements were performed using a QuantaMaster 40 spectrofluorometer (Photon Technology International) equipped with a Quantum Northwest TLC-50 temperature controller at 25.0 ± 0.05 °C.

*Fluorescence Titrations of Barbiturates **4a–d** with CF_3 Host (**3b**).* Stock solutions of **3b** (1.1 μM) and barbiturate (2.0 mM) in H_2O-saturated $CHCl_3$ were prepared separately. 1.8 mL of the host stock solution was combined with 200 μL of the guest stock solution to give a final guest–host solution containing 200 μM guest and 1 μM host. To a blank cuvette was added 1.5 mL of host stock and diluted with H_2O-saturated $CHCl_3$ to achieve a final concentration that matched that of the guest–host solution (1 μM). Aliquots of the guest–host solution were then added to the cuvette containing the host until minimal changes in the emission spectra were observed. Plots of F_{obs}/F_0 versus [Guest] were then fit to eq 1 using Origin to determine the association constant. This procedure was performed in triplicate, and the average K_a values and their standard deviations are reported.

$$\frac{F_{obs}}{F_0} = \frac{1 + (k_{HG}/k_H^0)K_a[G]}{1 + K_a[G]} \quad (1)$$

*Fluorescence Titrations of Hosts (**3b–e**) with Barbital.* Stock solutions of **3a–e** (2 μM) and barbital (2.0 mM) in H_2O-saturated $CHCl_3$ were prepared separately. 1.0 mL of the host stock solution was combined with 1 mL of the guest stock solution to give a final guest–host solution containing 1.0 mM guest and 1 μM host. To a blank cuvette was added 1.0 mL of host stock and diluted with H_2O-saturated $CHCl_3$ to achieve a final concentration that matched that of the guest–host solution (1 μM). Aliquots of the guest–host solution were then added to the cuvette containing the host until minimal changes in the emission spectra were observed. Plots of F_{obs}/F_0 versus [Guest] were then fit to eq 1 using Origin to determine the association constant. This procedure was performed in triplicate, and the average K_a values and their standard deviations are reported. Excitation (λ_{ex}) parameters for titration experiments were 321 (**3a**), 305 (**3b**, **3c**), 325 (**3d**), and 370 nm (**3e**).

*Fluorescence Titration of **3b** in the Presence of **4d** with Acetic Acid.* To a solution of 5 μM **3b** in H_2O-saturated $CDCl_3$ was added 100 equiv of **4d** (500 μM). Then aliquots of a dilute solution of acetic acid (10 mM) were added followed by the addition of aliquots of concentrated acetic acid and measurements using the following acquisition parameters: λ_{ex} = 325 nm; λ_{em} = 330–600 nm; excitation slits = 5.0 nm; integration time = 0.1 s; step size = 1 nm. The ratiometric response curve between 0 and 0.3 M is shown below.

*^1H NMR Titration of **3e** with **4b**.* A 1.0 mM solution of host **3e** in H_2O-saturated $CDCl_3$ was prepared. The host solution was then divided such that 560 μL was placed into an NMR tube and 2.0 mL was used to create a second solution containing 50 mM guest. An initial spectrum of the host was recorded using the following parameters: nt = 16 and d1 = 1 s, after which aliquots (1–25 μL total) of the guest solution were added until the N–H resonance of the host no longer shifted. The resultant chemical shifts were fit to obtain the K_a values for a 1:1 binding model. Similar procedures were used to obtain binding affinities for all host–guest K_a values reported.

Syntheses. *N-(6-Amino-4-bromopyridin-2-yl)-3,3-dimethylbutanamide (**1**).* A flame-dried flask containing 4-bromo-2,6-diaminopyridine (753 mg, 4.00 mmol) and anhydrous triethylamine (670 μL, 4.80 mmol) was charged with anhydrous THF (50 mL) and cooled to 0 °C. 3,3-Dimethylbutyryl chloride (560 μL, 4.03 mmol) was then added dropwise. The reaction mixture was warmed to room temperature and allowed to stir for 3 h. The crude reaction mixture was diluted with EtOAc (50 mL) and washed with water (3×) followed by brine (3×). The organic layer was then dried with $MgSO_4$, filtered, and concentrated via rotary evaporation. The crude product was purified via column chromatography (SiO_2, 1:1 EtOAc/Hex, R_f = 0.48) to yield a white solid (777 mg, 68%). ^1H NMR (500 MHz, $CDCl_3$) δ: 7.81 (s, 1H), 7.43 (s, 1H), 6.42 (s, 1H), 4.31 (s, 2H), 2.20 (s, 2H), 1.09 (s, 9H). $^{13}C\{^1H\}$ NMR (126 MHz, $CDCl_3$) δ: 170.30, 157.47, 150.43, 135.42, 107.14, 106.66, 51.87, 31.49, 29.92. HRMS (ES+ TOF) m/z: $[M + H]^+$ calcd for $C_{11}H_{17}BrN_3O$, 286.0555; found, 286.0556.

*N^1,N^3-Bis(4-bromo-6-(3,3-dimethylbutanamido)pyridin-2-yl)-isophthalamide (**2**).* A flame-dried flask containing **1** (900 mg, 3.14 mmol) and anhydrous triethylamine (500 μL, 3.58 mmol) was charged with anhydrous THF (40 mL) and cooled to 0 °C. Isophthaloyl chloride (325 mg, 1.60 mmol) in 5 mL of anhydrous THF (5 mL) was then added slowly. The reaction mixture was warmed to room temperature and allowed to stir for 23 h. The crude

DOI: 10.1021/acs.joc.9b00978
J. Org. Chem. 2019, 84, 8571–8577

reaction mixture was diluted with EtOAc and washed with water (3×) followed by brine (3×). The organic layer was then dried with $MgSO_4$, filtered, and concentrated via rotary evaporation. The crude product was purified via column chromatography (SiO_2, 1:1 EtOAc/Hex, R_f = 0.57) to yield a white solid (784 mg, 72%). ^{1}H NMR (500 MHz, $CDCl_3$) δ: 8.41 (s, 1H), 8.33 (s, 2H), 8.29 (s, 2H), 8.26 (s, 2H), 8.09 (d, J = 7.7 Hz, 2H), 7.66 (t, J = 7.7 Hz, 1H), 7.60 (s, 2H), 2.27 (s, 4H), 1.12 (s, 18H). ^{13}C{^{1}H} NMR (126 MHz, $CDCl_3$) δ: 170.51, 164.18, 150.14, 149.72, 136.59, 134.69, 131.04, 129.92, 126.07, 113.34, 112.95, 51.88, 31.58, 29.93. HRMS (ES+ TOF) m/z: $[M + H]^+$ calcd for $C_{30}H_{35}Br_2N_6O_4$, 701.1087; found, 701.1082.

*N^1,N^3-Bis(6-(3,3-dimethylbutanamido)-4-((4-nitrophenyl)-ethynyl)pyridin-2-yl)isophthalamide (**3a**).* A flame-dried flask containing **2** (96.9 mg, 0.138 mmol), $Pd(PPh_3)_4$ (7.6 mg, 6.6 μmol), and CuI (2.7 mg, 14 μmol) was equipped with a reflux condenser and evacuated/refilled with N_2 thrice. 4-Trifluoromethyl-phenylacetylene (63.6 mg, 0.43 mmol) was then added followed by a mixture of degassed, anhydrous THF/DIPA (10:1 mL). The solution was heated to reflux and monitored via ^{1}H NMR by observing the disappearance of the starting N−H protons. After 16 h, there was still a small amount of unreacted starting material; therefore, an additional aliquot of 4-nitrophenylacetylene (66 mg, 0.45 mmol) was added, and the reaction was continued to reflux for an additional 58 h. After this time, no further conversion was observed. The crude reaction mixture was cooled to room temperature, diluted with EtOAc, and filtered through Celite. The crude product was then dry-loaded onto silica and purified via column chromatography (SiO_2, 1:1 EtOAc/Hex) to yield an off-white solid (69 mg, 60%) containing a small amount of starting material impurity. Further purification was achieved using recycling GPC with a recycle time of 3.5 min. The crude material was collected on the 3rd cycle to yield the final product as a white solid (35 mg, 30%). ^{1}H NMR (500 MHz, DMSO-d_6) δ: 10.73 (s, 2H), 10.26 (s, 2), 8.54 (s, 1H), 8.30 (d, J = 7.9 Hz, 4H), 8.19 (d, J = 7.7 Hz, 2H), 8.07 (s, 2H), 8.01 (s, 2H), 7.97 (d, J = 8.0 Hz, 4H), 7.71 (t, J = 7.8 Hz, 1H), 2.35 (s, 4H), 1.03 (s, 18H). ^{13}C{^{1}H} NMR (126 MHz, DMSO-d_6) δ: 171.37, 165.61, 151.00, 150.75, 147.50, 134.02, 133.22, 132.50, 131.53, 128.87, 127.88, 127.74, 123.94, 112.08, 111.52, 91.43, 90.66, 48.99, 30.96, 29.55. HRMS (ES+ TOF) m/z: $[M + H]^+$ calcd for $C_{46}H_{43}N_8O_8$, 835.3198; found, 835.3224.

*N^1,N^3-Bis(6-(3,3-dimethylbutanamido)-4-((4-(trifluoromethyl)-phenyl)ethynyl)pyridin-2-yl)isophthalamide (**3b**).* A flame-dried flask containing **2** (98.9 mg, 0.140 mmol), $Pd(PPh_3)_4$ (8.3 mg, 7.2 μmol), and CuI (4.0 mg, 21 μmol) was equipped with a reflux condenser and evacuated/refilled with N_2 thrice. 4-Trifluoromethyl-phenylacetylene (70 μL, 0.43 mmol) was then added followed by a mixture of degassed, anhydrous THF/DIPA (10:1 mL). The solution was heated to reflux and monitored via ^{1}H NMR by observing the disappearance of the starting N−H protons. After 21 h, there was still a small amount of unreacted starting material; therefore, additional aliquots (2 total) of 4-trifluoromethylphenylacetylene (25 μL, 0.14 mmol) were added, and the reaction was continued to reflux for an additional 12 h. After this time, no further conversion was observed. The crude reaction mixture was cooled to room temperature, diluted with EtOAc, and filtered through Celite. The crude product was then dry-loaded onto silica and purified via column chromatography (SiO_2, 1:1 EtOAc/Hex) to yield an off-white solid (88 mg, 79%) containing a small amount of starting material impurity. Further purification was achieved using recycling GPC with a recycle time of 3.5 min. The crude material was collected on the 3rd cycle to yield the final product as a white solid (59 mg, 52%). ^{1}H NMR (500 MHz, DMSO-d_6) δ: 10.72 (s, 2H), 10.25 (s, 2H), 8.54 (s, 1H), 8.18 (d, J = 7.7 Hz, 2H), 8.05 (s, 2H), 7.99 (s, 2H), 7.91 (d, J = 8.0 Hz, 4H), 7.84 (d, J = 7.9 Hz, 4H), 7.71 (t, J = 7.7 Hz, 1H), 2.34 (s, 4H), 1.03 (s, 18H). ^{13}C{^{1}H} NMR (126 MHz, DMSO-d_6) δ: 171.4, 165.6, 151.0, 150.7, 134.1, 132.8, 132.7, 131.5, 129.1 (q, J = 28 Hz), 128.9, 127.7, 125.8 (q, J = 3.7 Hz), 125.7, 123.9 (q, J = 272 Hz), 112.0, 111.5, 91.1, 89.4, 49.0, 31.0, 29.6. ^{19}F NMR (471 MHz, DMSO-d_6) δ: −61.40. HRMS (ES+ TOF) m/z: $[M + H]^+$ calcd for $C_{48}H_{43}F_6N_6O_4$, 881.3250; found, 881.3272.

*N^1,N^3-Bis(6-(3,3-dimethylbutanamido)-4-(phenylethynyl)-pyridin-2-yl)isophthalamide (**3c**).* A flame-dried flask containing **2** (98.0 mg, 0.140 mmol), $Pd(PPh_3)_4$ (8.0 mg, 6.9 μmol), and CuI (3.2 mg, 17 μmol) was equipped with a reflux condenser and evacuated/refilled with N_2 thrice. Phenylacetylene (50 μL, 0.455 mmol) was then added followed by a mixture of degassed, anhydrous THF/DIPA (10:1 mL). The solution was heated to reflux and monitored until completion (6 h) via ^{1}H NMR by observing the disappearance of the starting N−H protons. The crude reaction mixture was cooled to room temperature, diluted with EtOAc, and filtered through Celite. The crude product was then dry-loaded onto silica and purified via column chromatography (SiO_2, 1:1 EtOAc/Hex) to yield an off-white solid. Further purification was achieved by recrystallization from a $CHCl_3$/Hex layering to yield the final product as a white solid (58 mg, 55%). ^{1}H NMR (500 MHz, DMSO-d_6) δ: 10.68 (s, 2H), 10.21 (s, 2H), 8.53 (s, 1H), 8.18 (d, J = 7.7 Hz, 2H), 8.01 (s, 2H), 7.95 (s, 2H), 7.71 (t, J = 7.8 Hz, 1H), 7.68 (d, J = 7.6 Hz, 4H), 7.54−7.43 (m, 6H), 2.34 (s, 4H), 1.03 (s, 18H). ^{13}C{^{1}H} NMR (126 MHz, DMSO-d_6) δ: 171.3, 165.6, 150.9, 150.7, 134.1, 133.4, 131.9, 131.5, 129.8, 128.9, 128.9, 127.7, 121.2, 111.9, 111.4, 92.9, 87.2, 49.0, 31.0, 29.6. HRMS (ES+ TOF) m/z: $[M + H]^+$ calcd for $C_{46}H_{45}N_6O_4$, 745.3502; found, 745.3514.

*N^1,N^3-Bis(6-(3,3-dimethylbutanamido)-4-((4-methoxyphenyl)-ethynyl)pyridin-2-yl)isophthalamide (**3d**).* A flame-dried flask containing **2** (98.9 mg, 0.140 mmol), $Pd(PPh_3)_4$ (8.6 mg, 7.4 μmol), CuI (3.8 mg, 20 μmol), and 4-methoxyphenylacetylene (40.0 mg, 0.30 mmol) was equipped with a reflux condenser and evacuated/refilled with N_2 thrice. Then a mixture of degassed, anhydrous THF/DIPA (10:1 mL) was added. The solution was heated to reflux and monitored until completion (7.5 h) via ^{1}H NMR by observing the disappearance of the starting N−H protons. The crude reaction mixture was cooled to room temperature, diluted with EtOAc, and filtered through Celite. The crude product was then dry-loaded onto silica and purified via column chromatography (SiO_2, 1:1 EtOAc/Hex) to yield an off-white solid (88 mg, 79%) containing a small amount of starting material impurity. Further purification was achieved using recycling GPC with a recycle time of 3.5 min. The crude material was collected on the 3rd cycle to yield the final product as a white solid (59 mg, 52%). ^{1}H NMR (500 MHz, DMSO-d_6) δ: 10.64 (s, 2H), 10.17 (s, 2H), 8.53 (s, 1H), 8.23−8.13 (m, 2H), 7.97 (s, 2H), 7.91 (s, 2H), 7.66−7.56 (m, 4H), 7.03 (d, J = 8.1 Hz, 4H), 3.82 (s, 6H), 2.33 (s, 4H), 1.03 (s, 18H). ^{13}C{^{1}H} NMR (126 MHz, DMSO-d_6) δ: 208.9, 203.2, 197.9, 188.5, 188.2, 171.7, 171.5, 171.3, 169.1, 166.5, 165.3, 152.2, 150.6, 149.4, 148.8, 131.0, 123.8, 93.0, 86.7, 68.6, 67.2. HRMS (ES+ TOF) m/z: $[M + H]^+$ calcd for $C_{48}H_{49}N_6O_6$, 805.3714; found, 805.3693.

*N^1,N^3-Bis(4-((4-(dimethylamino)phenyl)ethynyl)-6-(3,3-dimethylbutanamido)pyridin-2-yl)isophthalamide (**3e**).* A flame-dried flask containing **2** (98.4 mg, 0.140 mmol), $Pd(PPh_3)_4$ (9.2 mg, 8.0 μmol), CuI (3.1 mg, 16 μmol), and 4-dimethylaminophenylacetylene (61.0 mg, 0.42 mmol) was equipped with a reflux condenser and evacuated/refilled with N_2 thrice. Then a mixture of degassed, anhydrous THF/DIPA (10:1 mL) was added. The solution was heated to reflux and monitored until completion (5 h) via ^{1}H NMR by observing the disappearance of the starting N−H protons. The crude reaction mixture was cooled to room temperature, diluted with EtOAc, and filtered through Celite. The crude product was then dry-loaded onto silica and purified via column chromatography (SiO_2, 1:1 EtOAc/Hex) to yield a yellow solid (78 mg, 67%). ^{1}H NMR (500 MHz, DMSO-d_6) δ: 10.60 (s, 2H), 10.13 (s, 2H), 8.52 (s, 1H), 8.17 (d, J = 7.7 Hz, 2H), 7.93 (s, 2H), 7.86 (s, 2H), 7.70 (t, J = 7.7 Hz, 1H), 7.46 (d, J = 8.0 Hz, 4H), 6.74 (d, J = 8.1 Hz, 4H), 2.98 (s, 12H), 2.33 (s, 4H), 1.03 (s, 18H). ^{13}C{^{1}H} NMR (126 MHz, DMSO-d_6) δ: 171.2, 165.5, 150.8, 150.7, 150.5, 134.5, 134.1, 133.1, 131.4, 128.9, 127.6, 111.9, 111.5, 110.9, 106.9, 95.4, 85.8, 49.0, 30.9, 29.6. HRMS (ES+ TOF) m/z: $[M + H]^+$ calcd for $C_{50}H_{55}N_8O_4$, 831.4346; found, 831.4310.

DOI: 10.1021/acs.joc.9b00978
J. Org. Chem. 2019, 84, 8571−8577

■ ASSOCIATED CONTENT

Supporting Information

The Supporting Information is available free of charge on the ACS Publications website at DOI: 10.1021/acs.joc.9b00978.

NMR spectra, experimental data, titration data (PDF)

■ AUTHOR INFORMATION

Corresponding Author

*E-mail: pluth@uoregon.edu.

Notes

The authors declare no competing financial interest.

■ ACKNOWLEDGMENTS

This work was supported by NSF Grant CHE-1506221. The NMR and MS facilities in CAMCOR are supported through NSF awards CHE-0923589 and CHE-1625529. We thank Carolyn Levinn for assistance with revisions on this manuscript.

■ REFERENCES

(1) Cooke, G.; Rotello, V. M. Methods of modulating hydrogen bonded interactions in synthetic host-guest systems. *Chem. Soc. Rev.* **2002**, *31*, 275−286.

(2) Chang, S. K.; Hamilton, A. D. Molecular recognition of biologically interesting substrates: synthesis of an artificial receptor for barbiturates employing six hydrogen bonds. *J. Am. Chem. Soc.* **1988**, *110*, 1318−1319.

(3) Chang, S. K.; Van Engen, D.; Fan, E.; Hamilton, A. D. Hydrogen bonding and molecular recognition: synthetic, complexation, and structural studies on barbiturate binding to an artificial receptor. *J. Am. Chem. Soc.* **1991**, *113*, 7640−7645.

(4) McGrath, J. M.; Pluth, M. D. Understanding the Effects of Preorganization, Rigidity, and Steric Interactions in Synthetic Barbiturate Receptors. *J. Org. Chem.* **2014**, *79*, 711−719.

(5) McGrath, J. M.; Pluth, M. D. Linear Free Energy Relationships Reveal Structural Changes in Hydrogen-Bonded Host-Guest Interactions. *J. Org. Chem.* **2014**, *79*, 11797−11801.

(6) Hager, K.; Hartnagel, U.; Hirsch, A. Supramolecular dendrimers self-assembled from dendritic fullerene ligands and a homotritopic Hamilton receptor. *Eur. J. Org. Chem.* **2007**, 1942−1956.

(7) Li, Y.; He, Y.-M.; Li, Z.-W.; Zhang, F.; Fan, Q.-H. Supramolecular chiral dendritic monophosphites assembled by hydrogen bonding and their use in the Rh-catalyzed asymmetric hydrogenation. *Org. Biomol. Chem.* **2009**, *7*, 1890−1895.

(8) Binder, W. H.; Kunz, M. J.; Kluger, C.; Hayn, G.; Saf, R. Synthesis and Analysis of Telechelic Polyisobutylenes for Hydrogen-Bonded Supramolecular Pseudo-Block Copolymers. *Macromolecules* **2004**, *37*, 1749−1759.

(9) Binder, W. H.; Petraru, L.; Roth, T.; Groh, P. W.; Pálfi, V.; Keki, S.; Ivan, B. Magnetic and temperature-sensitive release gels from supramolecular polymers. *Adv. Funct. Mater.* **2007**, *17*, 1317−1326.

(10) Chen, S.; Mahmood, N.; Beiner, M.; Binder, W. H. Self-Healing Materials from V- and H-Shaped Supramolecular Architectures. *Angew. Chem., Int. Ed.* **2015**, *54*, 10188−10192.

(11) Bosch, S.; Zeininger, L.; Hauke, F.; Hirsch, A. A Supramolecular Approach for the Facile Solubilization and Separation of Covalently Functionalized Single- Walled Carbon Nanotubes. *Chem.-Eur. J.* **2014**, *20*, 2537−2541.

(12) Wessendorf, F.; Gnichwitz, J. F.; Sarova, G. H.; Hager, K.; Hartnagel, U.; Guldi, D. M.; Hirsch, A. Implementation of a hamiliton-receptor-based hydrogen-bonding motif toward a new electron donor-acceptor prototype: Electron versus energy transfer. *J. Am. Chem. Soc.* **2007**, *129*, 16057−16071.

(13) Wessendorf, F.; Grimm, B.; Guldi, D. M.; Hirsch, A. Pairing Fullerenes and Porphyrins: Supramolecular Wires That Exhibit Charge Transfer Activity. *J. Am. Chem. Soc.* **2010**, *132*, 10786−10795.

(14) Pagona, G.; Stergiou, A.; Gobeze, H. B.; Rotas, G.; D'Souza, F.; Tagmatarchis, N. Photoinduced charge separation in an oligophenylenevinylene-based Hamilton-type receptor supramolecularly associating two C_{60}-barbiturate guests. *Phys. Chem. Chem. Phys.* **2016**, *18*, 811−817.

(15) Ema, T.; Okuda, K.; Watanabe, S.; Yamasaki, T.; Minami, T.; Esipenko, N. A.; Anzenbacher, P., Jr. Selective Anion Sensing by Chiral Macrocyclic Receptors with Multiple Hydrogen-Bonding Sites. *Org. Lett.* **2014**, *16*, 1302−1305.

(16) Ema, T.; Tanida, D.; Sakai, T. Versatile and Practical Chiral Shift Reagent with Hydrogen-Bond Donor/Acceptor Sites in a Macrocyclic Cavity. *Org. Lett.* **2006**, *8*, 3773−3775.

(17) Ema, T.; Tanida, D.; Sakai, T. Versatile and Practical Macrocyclic Reagent with Multiple Hydrogen-Bonding Sites for Chiral Discrimination in NMR. *J. Am. Chem. Soc.* **2007**, *129*, 10591−10596.

(18) Aoki, I.; Kawahara, Y.; Sakaki, T.; Harada, T.; Shinkai, S. Molecular Design of a New Fluorescent Barbiturate Receptor. Sensitive Detection of Barbiturates through Solvent Extraction. *Bull. Chem. Soc. Jpn.* **1993**, *66*, 927−933.

(19) Chambers, R.C.; Bell, E. J.; Records, T. M.; Cherian, A.; Ragan, K.; Swartout, B. Cholesteric liquid crystal displays as optical sensors of barbiturate binding. *Liq. Cryst.* **2007**, *34*, 1221−1226.

(20) Westwood, J.; Coles, S. J.; Collinson, S. R.; Gasser, G.; Green, S. J.; Hursthouse, M. B.; Light, M. E.; Tucker, J. H. R. Binding and Electrochemical Recognition of Barbiturate and Urea Derivatives by a Regioisomeric Series of Hydrogen-Bonding Ferrocene Receptors. *Organometallics* **2004**, *23*, 946−951.

(21) Young, M. C.; Liew, E.; Hooley, R. J. Colorimetric barbiturate sensing with hybrid spin crossover assemblies. *Chem. Commun.* **2014**, *50*, 5043−5045.

(22) Kondo, S.-i.; Endo, K.; Iioka, J.; Sato, K.; Matsuta, Y. UV-vis and fluorescence detection by receptors based on an isophthalamide bearing a phenylethynyl group. *Tetrahedron Lett.* **2017**, *58*, 4115−4118.

(23) Seidenkranz, D. T.; McGrath, J. M.; Zakharov, L. N.; Pluth, M. D. Supramolecular bidentate phosphine ligand scaffolds from deconstructed Hamilton receptors. *Chem. Commun.* **2017**, *53*, 561−564.

(24) Spitler, E. L.; Shirtcliff, L. D.; Haley, M. M. Systematic structure - property investigations and ion-sensing studies of pyridine-derivatized donor/acceptor tetrakis(arylethynyl)benzenes. *J. Org. Chem.* **2007**, *72*, 86−96.

(25) Wilson, J. N.; Bunz, U. H. F. Switching of intramolecular charge transfer in cruciforms: Metal ion sensing. *J. Am. Chem. Soc.* **2005**, *127*, 4124−4125.

(26) Lakowicz, J. R. Solvent and Environmental Effects. In *Principles of Fluorescence Spectroscopy*; Springer US: Boston, MA, 2006; pp 205−235.

DOI: 10.1021/acs.joc.9b00978
J. Org. Chem. 2019, 84, 8571−8577